PHYSICAL REVIEW A VOLUME 24, NUMBER 1 JULY 1981

Widths and fluorescence yields of atomic L-shell vacancy states

Mau Hsiung Chen and Bernd Crasemann
Department of Physics and Chemical Physics Institute, University of Oregon, Eugene, Oregon 97403

Hans Mark
Department of the Air Force, Washington, D. C. 20330

(Received 9 February 1981)

A comprehensive set of theoretical L-shell Auger and total widths, and Coster-Kronig and fluorescence yields is presented for atomic numbers $18 \leq Z \leq 100$. These quantities are based on *ab initio* relativistic calculations. Agreement with experimental values is fair for ω_1 and generally good for ω_2, ω_3 ($Z \geq 54$), f_{23} ($Z \geq 60$), $\Gamma(L_2)$, $\Gamma(L_3)$, and for $\Gamma(L_1)$ in the range $49 \leq Z \leq 75$. Discrepancies in $\Gamma(L_1)$ for $Z < 49$ point toward the need for a many-body calculation of low-energy $L_1 - L_{2,3}M_{4,5}$ Coster-Kronig transitions. There is a pronounced need for measurements of ω_3 and f_{23} of elements lighter than Xe.

I. INTRODUCTION

The state of an atom that contains a deep-lying vacancy has the following gross properties of main practical importance[1]:

(i) The *mean life* τ, and the *width* $\Gamma = \hbar/\tau$. The mean life is conveniently expressed in femtoseconds or in atomic units of time (1 a.u. $= 2.4189 \times 10^{-17}$ s). The width is usually given in electron volts or in atomic units of energy (1 a.u. $= 1$ hartree $= 27.2117$ eV); it is proportional to the decay probability per unit time ($1\ \text{eV}/\hbar = 1.5193 \times 10^{15}\ \text{s}^{-1} = 3.6749 \times 10^{-2}$ a.u.$^{-1}$). The width of a vacancy state represents the sum of decay probabilities through many (usually 10^2–10^4) channels.

(ii) The *partial widths* Γ_R for radiative decay, Γ_A for Auger decay, and Γ_{CK} for Coster-Kronig decay, and the ratio $\omega = \Gamma_R/\Gamma$ known as the *fluorescence yield*. We have

$$\Gamma \cong \Gamma_R + \Gamma_A + \Gamma_{CK} \tag{1}$$

for a free atom, if we neglect other, improbable modes of decay.

(iii) Coster-Kronig transitions[2] can very much shorten the lifetimes of atomic inner-shell vacancies; these are radiationless transitions in which a vacancy "bubbles up" among the subshells of a major shell. Due to large wave-function overlap among the pertinent hole states, Coster-Kronig transitions tend to be exceedingly intense[3] and hence govern the lifetimes of those states for which they are possible. Quantities of interest are therefore the *Coster-Kronig yields* f_{ij} which describe the probability that a vacancy is shifted from subshell i to subshell j of the same major shell.

Vacancy lifetimes are of interest in diverse contexts, ranging from beam-foil spectroscopy to laser design. Fluorescence yields determine the intensity of x-ray emission from ionized atoms, and hence have applications in such areas as fluorescence analysis,[4] astrophysics,[4] medical physics,[5] and wherever one performs calculations of energy transport through matter under the impact of radiation. Coster-Kronig yields are required to calculate x-ray spectra[6] and to compute branching ratios in the deexcitation cascade, e.g., to predict the final-charge state of atoms following deexcitation of a deep-lying initial vacancy.[7]

In this paper we present a comprehensive set of theoretical L-shell Auger and total widths and Coster-Kronig and fluorescence yields, for atomic numbers $18 \leq Z \leq 100$. These quantities are based on *ab initio* relativistic calculations. The radiative transition probabilities were computed by Scofield[8,9]; some of the radiationless transition probabilities were previously calculated by our group,[3,10,11] and were supplemented by additional, new computations. We compare the results with those of earlier, nonrelativistic calculations,[12,13] with Krause's semiempirical fits,[14,15] and with recent experimental data.

II. THEORY

The relativistic Auger transition rates were calculated from perturbation theory, assuming frozen orbitals.[10] In the j-j coupling scheme, the total transition rate from an initial j_1' hole state to a final $j_1 j_2$ two-hole configuration, in atomic units, is given by

$$\Gamma = \frac{1}{2j_1'+1} \sum_{j_2'} \sum_{JM} \sum_{J'M'} |\langle j_1' j_2' J'M' | V_{12} | j_1 j_2 JM \rangle|^2 . \tag{2}$$

Here $\langle j_1' j_2' J'M' |$ represents the j-j coupled state of the initial L-shell hole and the hole in the continuum, while $\langle j_1 j_2 JM |$ describes the final two-hole state. The continuum wave function with total angular momentum j_2' is normalized to represent

one electron ejected per unit time. While relativistic calculations are naturally performed in j-j coupling, the coupling scheme is immaterial if one considers the intensities of groups of transitions that include all possible j-j configurations which correspond to a given LS configuration; this is the case in the present work.

For the two-electron operator V_{12} we choose Møller's operator, which is suitable for the local-potential approximation[16,17] underlying the Dirac-Hartree-Slater (DHS) wave functions used in the present work. The Møller operator is

$$V_{12}=(1-\vec{\alpha}_1\cdot\vec{\alpha}_2)e^{i\omega r_{12}}/r_{12}, \tag{3}$$

where the $\vec{\alpha}_i$ are Dirac matrices, and ω is the wave number of the virtual photon.

The relativistic matrix elements of Eq. (2) can be separated into angular and radial parts. Details of the calculation are provided in Ref. 10.

The Coster-Kronig energies, which greatly affect the transition rates (especially near cutoff), were found by calculating the expectation of the Hamiltonian with DHS wave functions. A first-order correction to the local approximation was thus made. We have allowed for complete relaxation by performing separate calculations for the initial one-hole and the final two-hole states of the atom. Quantum-electrodynamic corrections were incorporated in the energy calculations.[11]

Auger transition energies are less critical than those of Coster-Kronig processes. The Auger energies could therefore be calculated from relativistic relaxed-orbital binding energies for neutral atoms,[18] using the "$Z+1$ rule" to allow for the effect of the second vacancy in the final state.[1] This approach introduces an error of ~30 eV in the Auger energies, which has been found to have negligible effect on the transition rates.

Computation of the radiationless transition rates was performed with DHS wave functions,[18,19] employing a general relativistic Auger program developed in our previous work.[10] Radiative decay rates for the computation of total widths and fluorescence yields were taken from the relativistic work of Scofield.[8,9,20]

III. RESULTS AND DISCUSSION

Theoretical L-shell Auger and total widths and Coster-Kronig and fluorescence yields are listed in Tables I and II. In Figs. 1–3, we compare our calculated relativistic L-subshell fluorescence yields with results from McGuire's nonrelativistic approximate Herman-Skillman calculations[13] and with experimental data compiled by Krause.[14] The L_1 fluorescence yields as a function of Z display discontinuities caused by the onset or cutoff of the

TABLE I. Theoretical L_1 subshell Auger widths $\Gamma_A(L_1)$ and total widths $\Gamma(L_1)$ (in eV), Coster-Kronig yields f_{12} and f_{13}, and fluorescence yields ω_1.

Element	$\Gamma_A(L_1)$	$\Gamma(L_1)$	f_{12}	f_{13}	ω_1[a]
$_{18}$Ar	0.121	2.716	0.327	0.628	1.078(−4)
$_{20}$Ca	0.173	3.495	0.327	0.623	1.963(−4)
$_{25}$Mn	0.277	6.435	0.268	0.688	3.47(−4)
$_{30}$Zn	0.477	9.597	0.284	0.666	6.02(−4)
$_{35}$Br	0.712	8.496	0.190	0.725	1.73(−3)
$_{36}$Kr	0.760	7.944	0.198	0.704	2.21(−3)
$_{40}$Zr	0.941	5.910	0.088	0.747	5.50(−3)
$_{45}$Rh	1.150	6.768	0.062	0.759	9.16(−3)
$_{47}$Ag	1.238	6.852	0.068	0.740	0.0114
$_{50}$Sn	1.360	3.002	0.188	0.322	0.0365
$_{52}$Te	1.436	3.265	0.192	0.326	0.0417
$_{54}$Xe	1.510	3.524	0.196	0.328	0.0475
$_{56}$Ba	1.580	3.790	0.200	0.329	0.0538
$_{60}$Nd	1.674	4.268	0.209	0.331	0.0678
$_{63}$Eu	1.740	4.654	0.214	0.333	0.0793
$_{67}$Ho	1.811	5.185	0.218	0.336	0.0964
$_{70}$Yb	1.864	5.349	0.116	0.352	0.116
$_{74}$W	1.951	5.959	0.185	0.350	0.137
$_{80}$Hg	2.086	14.471	0.069	0.705	0.082
$_{83}$Bi	2.154	14.743	0.0549	0.700	0.0988
$_{90}$Th	2.314	15.761	0.0575	0.656	0.140
$_{92}$U	2.359	16.514	0.051	0.656	0.150
$_{96}$Cm	2.445	16.929	0.047	0.629	0.180
$_{98}$Cf	2.488	17.234	0.047	0.612	0.197
$_{100}$Fm	2.534	17.536	0.047	0.593	0.216

[a] Numbers in parentheses signify powers of ten, e.g., $1.078(-4)=1.078\times10^{-4}$.

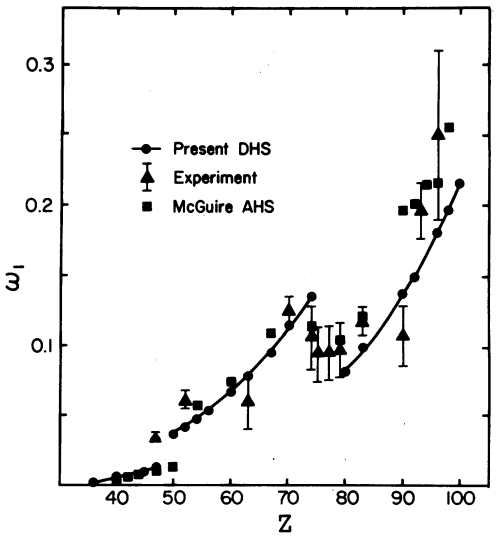

FIG. 1. Theoretical relativistic DHS L_1-subshell fluorescence yields ω_1, as function of atomic number Z. Experimental data (collected in Ref. 14) and the nonrelativistic results of McGuire's approximate Hartree-Slater (AHS) calculation (Ref. 13) are also shown.

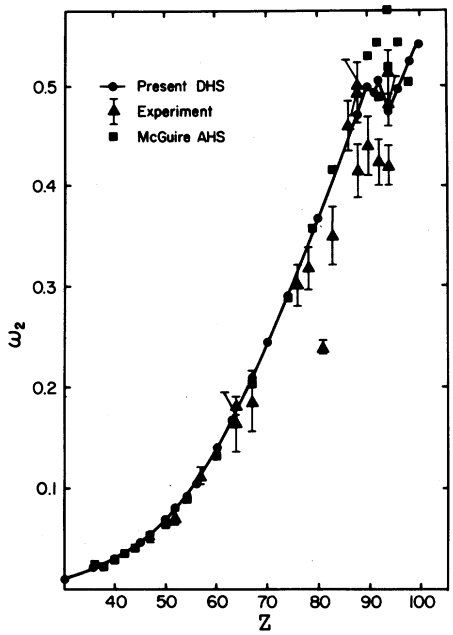

FIG. 2. Theoretical relativistic DHS L_2-subshell fluorescence yields ω_2, as function of atomic number Z. Experimental data (collected in Ref. 14) and the nonrelativistic results of McGuire's approximate Hartree-Slater (AHS) calculation (Ref. 13) are also indicated.

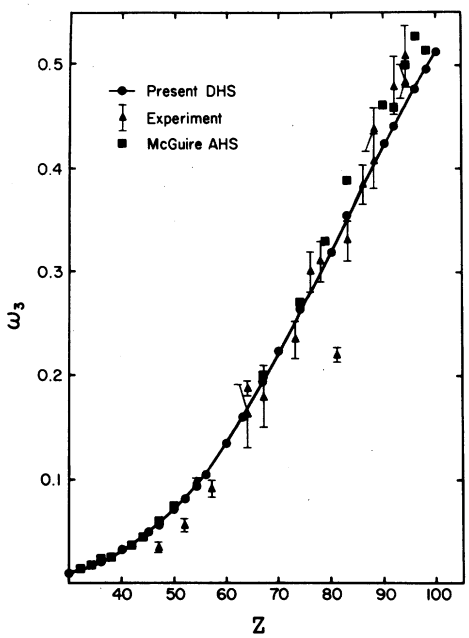

FIG. 3. Theoretical relativistic DHS L_3-subshell fluorescence yields ω_3, as function of atomic number Z. Experimental data (collected in Ref. 14) and the nonrelativistic results of McGuire's approximate Hartree-Slater (AHS) calculation (Ref. 13) are also shown.

TABLE II. Theoretical L_2 and L_3 subshell Auger widths $\Gamma_A(L_2)$ and $\Gamma_A(L_3)$ and total widths $\Gamma(L_2)$ and $\Gamma(L_3)$ (in eV), Coster-Kronig yields f_{23}, and fluorescence yields ω_2 and ω_3.

Element	$\Gamma_A(L_2)$	$\Gamma(L_2)$	f_{23}	ω_2	$\Gamma_A(L_3)$	$\Gamma(L_3)$	ω_3[a]
$_{18}$Ar					0.155	0.155	1.82(−4)
$_{20}$Ca					0.210	0.210	2.85(−4)
$_{25}$Mn	0.390	0.392		0.0039	0.337	0.339	4.57(−3)
$_{30}$Zn	0.664	0.691		0.0114	0.689	0.697	0.0112
$_{36}$Kr	1.101	1.245	0.095	0.0211	1.167	1.193	0.0216
$_{40}$Zr	1.373	1.628	0.126	0.0307	1.465	1.514	0.0320
$_{45}$Rh	1.705	2.132	0.152	0.0478	1.860	1.958	0.0501
$_{47}$Ag	1.832	2.323	0.155	0.056	2.028	2.152	0.0577
$_{50}$Sn	2.016	2.637	0.166	0.070	2.256	2.432	0.0723
$_{52}$Te	2.128	2.843	0.171	0.081	2.406	2.623	0.0829
$_{54}$Xe	2.236	3.049	0.174	0.093	2.557	2.823	0.0942
$_{56}$Ba	2.336	3.255	0.177	0.105	2.696	3.018	0.107
$_{60}$Nd	2.456	3.552	0.170	0.139	2.897	3.353	0.136
$_{63}$Eu	2.534	3.778	0.162	0.167	3.041	3.622	0.160
$_{67}$Ho	2.611	4.092	0.152	0.210	3.211	3.994	0.196
$_{70}$Yb	2.662	4.358	0.143	0.246	3.340	4.306	0.224
$_{74}$W	2.753	4.821	0.139	0.290	3.543	4.812	0.264
$_{80}$Hg	2.877	5.696	0.127	0.368	3.878	5.704	0.320
$_{83}$Bi					4.051	6.271	0.354
$_{88}$Ra	3.028	7.243	0.110	0.472			
$_{90}$Th	3.060	7.712	0.106	0.498	4.464	7.738	0.423
$_{91}$Pa	3.070	8.338	0.138	0.494			
$_{92}$U	3.082	8.620	0.138	0.505	4.571	8.204	0.443
$_{94}$Pu	3.103	10.259	0.225	0.473			

TABLE II. (*Continued*).

Element	$\Gamma_A(L_2)$	$\Gamma(L_2)$	f_{23}	ω_2	$\Gamma_A(L_3)$	$\Gamma(L_3)$	ω_3[a]
$_{96}$Cm	3.126	10.708	0.211	0.497	4.805	9.189	0.477
$_{98}$Cf	3.146	11.261	0.196	0.524	4.934	9.761	0.494
$_{100}$Fm	3.168	12.118	0.199	0.539	5.060	10.365	0.512

[a] Numbers in parentheses signify powers of ten, e.g., $1.82(-4) = 1.82 \times 10^{-4}$.

L_1-$L_{2,3}$ Coster-Kronig transitions (Fig. 1).[11] There is only fair agreement between measured and calculated fluorescence yields ω_1.

The L_2 fluorescence yields drop at $Z = 91$ because of the onset of L_2-L_3M_5 Coster-Kronig transitions, and at $Z = 94$ because at this atomic number L_2-L_3M_4 Coster-Kronig transition become energetically possible (Fig. 2). For L_2 and L_3 fluorescence yields, our present DHS results agree quite well with experimental data, except for ω_3 below $Z = 54$ (Fig. 3). Here, the only two available measurements fall significantly below calculated fluorescence yields. Additional measurements would be desirable before any special significance is ascribed to this discrepancy.

L_2-shell Coster-Kronig yields f_{23} are plotted in Fig. 4. The jumps in f_{23} at $Z = 91$ and 94 are due to the onsets of L_2-L_3M_5 and L_2-L_3M_4 Coster-Kronig transitions, respectively. Theory and experiment are found to agree well above $Z = 60$.

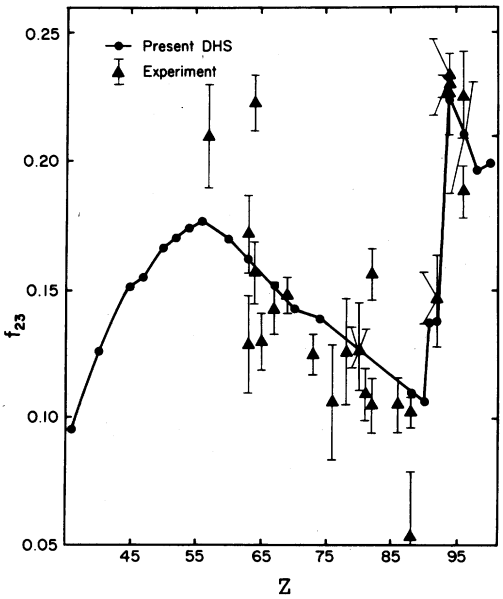

FIG. 4. L_2-subshell Coster-Kronig yields f_{23} from the present relativistic DHS calculation, as function of atomic number. Experimental data (collected in Ref. 14) are shown for comparison.

No experimental data are available below $Z = 56$.

L-subshell widths are shown in Figs. 5–7, compared with nonrelativistic results,[13] Krause and Oliver's semiempirical fit,[15] and experimental values.[15,21] In general, the present relativistic widths agree better than earlier nonrelativistic results[13] with the semiempirical fits.[15] The agreement between DHS and semiempirical widths is quite good over the entire range of atomic numbers for $\Gamma(L_2)$ and $\Gamma(L_3)$. For L_1-hole states, we find good agreement between relativistically calculated and semiempirically fitted widths in the range of atomic numbers from $Z = 49$ to $Z = 75$ (Fig. 5). The pronounced discrepancies outside of this range can be ascribed to the fact that here the intense L_1-$L_{2,3}M_{4,5}$ Coster-Kronig transitions are energetically possible.[11] For heavy elements, the

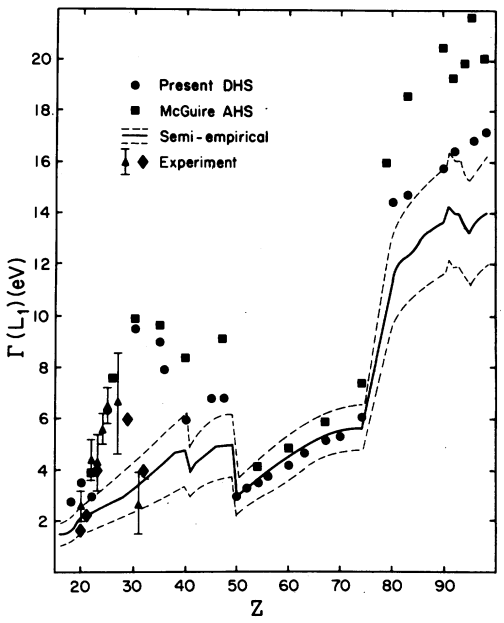

FIG. 5. Theoretical relativistic DHS L_1-subshell total widths $\Gamma(L_1)$ as function of atomic number. Also shown are results of McGuire's nonrelativistic approximate Hartree-Slater (AHS) calculation (Ref. 13), experimental data (collected in Ref. 15), and the semiempirical fit of Krause and Oliver (Ref. 15) (solid line) with its estimated uncertainties indicated by broken curves.

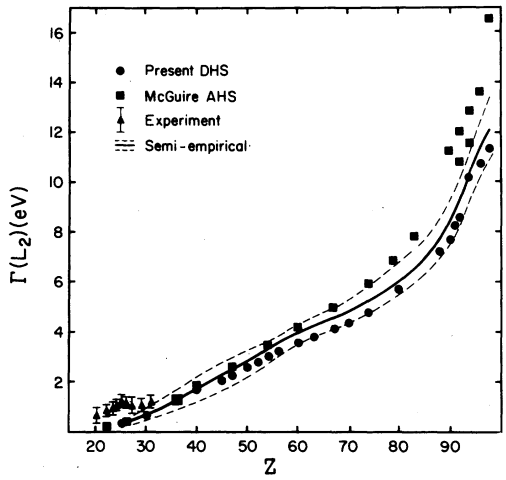

FIG. 6. Theoretical relativistic DHS L_2-subshell total widths $\Gamma(L_2)$ as function of atomic number Z. Also shown are results of McGuire's nonrelativistic approximate Hartree-Slater (AHS) calculation (Ref. 13), experimental data (collected in Ref. 15), and the semi-empirical fit of Krause and Oliver (Ref. 15) (solid curve) with its estimated uncertainties indicated by broken curves.

present theory overestimates L_1-$L_{2,3}M_{4,5}$ rates by ~10%, while for $27 < Z < 50$ the discrepancy can be as large as a factor of 3. To resolve this serious problem, a many-body calculation of low-energy L_1-$L_{2,3}M_{4,5}$ Coster-Kronig transitions would be desirable.

Solid-state effects and exchange splitting can also contribute to discrepancies between calculated free-atom hole-state widths and measurements. For $Z < 30$, L_2-$L_3M_{4,5}$ Coster-Kronig transitions should be energetically impossible according to free-atom calculations with DHS wave functions including relaxation and quantum electrodynamic (QED) corrections,[11] but experiments[22] indicate that these transitions do occur in solids because of the contribution from extra-atomic relaxation. Consequently, L_2-hole-state widths in solids are larger than for isolated atoms with atomic numbers $20 < Z < 30$. In this same range of atomic numbers, $\Gamma(L_2)$ for certain elements contains a contribution from exchange splitting.[23] For L_3-hole states as well, discrepancies between theory and experiment for $20 < Z < 30$ are likely to be due in part to contributions from exchange splitting.[23]

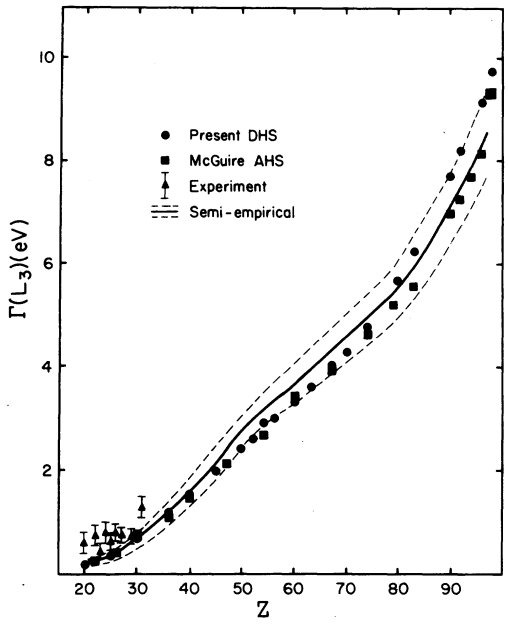

FIG. 7. Theoretical relativistic DHS L_3-subshell total widths $\Gamma(L_3)$ as function of atomic number Z. Also shown are results of McGuire's nonrelativistic approximate Hartree-Slater (AHS) calculation (Ref. 13), experimental data (collected in Ref. 15), and the semi-empirical fit of Krause and Oliver (Ref. 15) (solid curve) with its estimated uncertainties indicated by broken curves.

IV. CONCLUSION

Atomic level widths and fluorescence yields have applied and technological relevance; they also constitute gross hole-state properties that can be measured and serve to test sums of theoretical transition-rate calculations. The most refined individual-particle calculations, which include relativity and QED, agree well with the sparse experimental results over limited ranges of atomic numbers; on the other hand, major discrepancies point toward the need for many-body calculations and a better understanding of solid-state effects, as well as for additional experiments.

ACKNOWLEDGMENT

This work was supported in part by the U. S. Air Force Office of Scientific Research through Grant No. 79-0026.

[1]W. Bambynek, B. Crasemann, R. W. Fink, H.-U. Freund, H. Mark, C. D. Swift, R. E. Price, and P. Venugopala Rao, Rev. Mod. Phys. 44, 716 (1972).
[2]D. Coster and R. de L. Kronig, Physica 2, 13 (1932).
[3]M. H. Chen, B. Crasemann, and H. Mark, At. Data Nucl. Data Tables 24, 13 (1979).
[4]T. E. Bunch, L. J. Caroff, and H. Mark, in *Atomic Inner-Shell Processes*, edited by B. Crasemann (Academic, New York, 1975), Vol. II, p. 187.
[5]L. T. Dillman and F. C. Von de Lage, MIRD Pamphlet

No. 10 (Society of Nuclear Medicine, New York, 1975).
[6]M. H. Chen, B. Crasemann, M. Aoyagi, and H. Mark, Phys. Rev. A 15, 2312 (1977).
[7]B. F. Rozsnyai, V. L. Jacobs, and J. Davis, Phys. Rev. A 21, 1798 (1980).
[8]J. H. Scofield, Phys. Rev. A 10, 1507 (1974).
[9]J. H. Scofield, At. Data Nucl. Data Tables 14, 121 (1974).
[10]M. H. Chen, E. Laiman, B. Crasemann, M. Aoyagi, and H. Mark, Phys. Rev. A 19, 2253 (1979).
[11]M. H. Chen, B. Crasemann, K.-N. Huang, M. Aoyagi, and H. Mark, At. Data Nucl. Data Tables 19, 97 (1977).
[12]E. J. McGuire, in *Atomic Inner-Shell Processes*, edited by B. Crasemann (Academic, New York, 1975), Vol. I, p. 293.
[13]E. J. McGuire, Phys. Rev. A 3, 587 (1971); in *Proceedings of the International Conference on Inner-Shell Ionization Phenomena and Future Applications*, edited by R. W. Fink, S. T. Manson, J. M. Palms, and P. Venugopala Rao [U. S. Atomic Energy Commission Report No. CONF-720404 (unpublished)], Vol. I, p. 662.
[14]M. O. Krause, J. Phys. Chem. Ref. Data 8, 307 (1979).
[15]M. O. Krause and J. H. Oliver, J. Phys. Chem. Ref. Data 8, 328 (1979).
[16]K.-N. Huang, J. Phys. B 11, 787 (1978).
[17]J. B. Mann and W. R. Johnson, Phys. Rev. A 4, 41 (1971).
[18]K.-N. Huang, M. Aoyagi, M. H. Chen, B. Crasemann, and H. Mark, At. Data Nucl. Data Tables 18, 243 (1976).
[19]D. A. Liberman, D. T. Cromer, and J. T. Waber, Comput. Phys. Commun. 2, 107 (1971).
[20]J. H. Scofield, in *Atomic Inner-Shell Processes*, edited by B. Crasemann (Academic, New York, 1975), Vol. I, p. 265.
[21]B. E. Gnade, R. A. Braga, and R. W. Fink, Phys. Rev. C 21, 2025 (1980); 23, 580 (E) (1981).
[22]L. I Yin, I. Adler, M. H. Chen, and B. Crasemann, Phys. Rev. A 7, 897 (1973).
[23]J. C. Fuggle and S. F. Alvarado, Phys. Rev. A 22, 1615 (1980).